



Monitoring the COVID-19 immune landscape in Japan

Misaki Sasanami, Taishi Kayano, Hiroshi Nishiura*

Kyoto University School of Public Health, Yoshida-Konoe, Sakyo, Kyoto 606-8601, Japan

ARTICLE INFO

Article history:
Received 22 April 2022
Revised 2 June 2022
Accepted 3 June 2022

Keywords:
COVID-19
Vaccination
Epidemiology
Mathematical model
Statistical model

ABSTRACT

Objectives: COVID-19 vaccination in Japan started on February 17, 2021. Because the timing of vaccination and the risk of severe COVID-19 greatly varied with age, the present study aimed to monitor the age-specific fractions of the population who were immune to SARS-CoV-2 infection after vaccination.

Methods: Natural infection remained extremely rare, accounting for less than 5% of the population by the end of 2021; thus, we ignored natural infection-induced immunity and focused on vaccine-induced immunity. We estimated the fraction of the population immune to infection by age group using vaccination registry data from February 17, 2021, to October 17, 2021. We accounted for two important sources of delay: (i) reporting delay and (ii) time from vaccination until immune protection develops.

Results: At the end of the observation period, the proportion of individuals still susceptible to SARS-CoV-2 infection substantially varied by age and was estimated to be $\geq 90\%$ among people aged 0–14 years, in contrast to approximately 20% among the population aged ≥ 65 years. We also estimated the effective reproduction number over time using a next-generation matrix while accounting for differences in the proportion immune to infection by age.

Conclusion: The COVID-19 immune landscape greatly varied by age, and a substantial proportion of young adults remained susceptible. Vaccination contributed to a marked decrease in the reproduction number.

© 2022 The Authors. Published by Elsevier Ltd on behalf of International Society for Infectious Diseases. This is an open access article under the CC BY-NC-ND license (<http://creativecommons.org/licenses/by-nc-nd/4.0/>)

Introduction

Since the COVID-19 epidemic spread on a global scale in 2020, it considerably altered daily life. With the hope of mitigating the COVID-19 risk, vaccination campaigns began in December 2020 in many countries, often using a prioritization vaccination strategy (Haas et al., 2021; Hall et al., 2021; Jentsch et al., 2021; Mathieu et al., 2021; Sasanami et al., 2022; Thompson et al., 2021). Mass vaccination campaigns occurred primarily when the original (wild-type) strain, the Alpha variant (B.1.1.7), the Beta variant (B.1.351), or other variants were dominant in circulation and against which the available vaccines provided substantial protection (Chemaitelly et al., 2021; Chung et al., 2021; Dagan et al., 2021; Haas et al., 2021; Hall et al., 2021; Pritchard et al., 2021). However, additional variants of concern have since been reported, including the Delta variant (B.1.617) and the highly transmissible Omicron variant (B.1.1.529) (Belay and Godfred-Cato, 2022; Elbe and Buckland-Merrett, 2017; GISAID, 2022; Houhamdi et al.,

2022; Loconsole et al., 2022; Nyberg et al., 2022; Ramírez et al., 2022; Veneti et al., 2022). The effectiveness of the widely used messenger RNA (mRNA) vaccines to prevent infection has been notably low against the presently widespread Omicron variant (Andrews et al., 2022; Ferdinands et al., 2022; Tseng et al., 2022).

In Japan, there were three eligibility categories for receiving a COVID-19 vaccination: (1) healthcare workers, (2) the general population, and (3) university students and staff and company employees. Healthcare workers were prioritized as the first group and began receiving vaccinations on February 17, 2021, and the general population ≥ 65 years became eligible on April 12, 2021. The eligible age groups were sequentially expanded in a descending manner. To receive a vaccination, individuals needed to present a vaccination coupon that they had received from the city council that arranged the vaccination program for the local population. Alongside the general population vaccination program, which used the mRNA vaccine BNT162b2, the university and workplace vaccination program started on June 21, 2021, and was arranged by universities/colleges and companies voluntarily and administered the mRNA-1273 vaccine. The importance of vaccination was particularly emphasized when the Delta variant became dominant in Japan in mid-May 2021 (National Institute of Infectious Dis-

* Corresponding author: Hiroshi Nishiura, Kyoto University School of Public Health, Yoshida-Konoe, Sakyo, Kyoto 606-8601, Japan Tel: +81 75 753 4456; Fax: +81 75 753 4458.

E-mail address: nishiura.hiroshi.5r@kyoto-u.ac.jp (H. Nishiura).

eases, 2021). At this time, the country was preparing to host the Tokyo Olympic Games in late July.

To record the dispatched and administered doses, the Japanese government developed the Vaccination System (V-SYS) and the Vaccination Record System (VRS). The V-SYS records allocated doses (in contrast with actually administered doses), whereas the VRS registers doses administered to those who showed a vaccination coupon upon vaccination; the VRS also records the vaccinee's age. As such, not all healthcare workers were recorded in the VRS because some were vaccinated before the city councils sent them vaccination coupons. In addition, there was a substantial reporting delay in the VRS, particularly for those who were vaccinated through the university and workplace vaccination programs. This reporting delay was mostly because many of these people were young and therefore had not yet received a municipal vaccination coupon by the time they were vaccinated under the university or workplace vaccination program. Their vaccination was later reported when their vaccination coupons were issued.

Japan experienced less than 5% of the cumulative risk of confirmed COVID-19 cases by the end of 2021 (Ministry of Health, Labor and Welfare, 2021a). Thus, it has been vital for Japan to vaccinate as many people as possible. To understand the immune landscape at single points in time, seroepidemiological surveys have been conducted in various settings (Berselli et al., 2022; Madhi et al., 2022; Nopsopon et al., 2021; Slot et al., 2020; Xu et al., 2020), but the required time and cost of these surveys constrain the continuous implementation of such labor-intensive studies. The purpose of the present study was to develop a method to enable real-time monitoring of the COVID-19 immune landscape using available vaccination surveillance data. The impact of the immune landscape on the reproduction number over time was also examined.

Materials and methods

Vaccine registry data

The VRS and V-SYS do not report the total number of vaccinees, therefore, we used the two datasets to complement each other. The VRS data were obtained from the Ministry of Health, Labor and Welfare (Supplementary data 1), and the V-SYS data were obtained from the website of the Prime Minister's Office of Japan. From V-SYS, we obtained the number of doses allocated to healthcare workers, university students/staff, and company employees between February 17, 2021, and October 10, 2021. Information on the vaccinees' age was unavailable in V-SYS, and it recorded healthcare workers only up to July 30, 2021. From the VRS data, we obtained the number of daily administered doses between April 17, 2021, and October 17, 2021. The number of new vaccinees was recorded in the VRS, and those not previously reported in the past weeks were added over time. In addition, we used national census data for the Japanese population and working population age distributions. These datasets were retrieved from the Statics Bureau of Japan.

Statistical model

We first estimated the number of vaccinated people based on the programs, categorizing vaccinees into five age groups ($n_a = 5$): 0–14, 15–29, 30–44, 45–64, and ≥ 65 years. In doing so, the reporting delay in the VRS data was taken into consideration. We then calculated the fraction of people susceptible to SARS-CoV-2 infection and accounted for the delay during which vaccinated individuals develop immunity. The impacts of vaccination were quantified by examining time-varying reproduction numbers using the next-generation matrix (NGM). Hereafter, “immune” refers to individuals

protected from SARS-CoV-2 infection regardless of manifestation of COVID-19 symptoms.

First doses allocated to healthcare workers

We mainly used the V-SYS data because not all vaccinated healthcare workers were recorded in the VRS. However, because the V-SYS does not record age, we calculated the number of daily doses distributed to each age group by assuming that their age distribution was identical to that recorded in the VRS.

First doses administered to the general population, university students/staff, and company employees

The VRS data were used to estimate the number of people vaccinated through the general, university, and workplace vaccination programs, while the reporting delay was quantified and taken into consideration. We also added the number of underreported vaccinees from the V-SYS data.

2.2.2. Estimating the number of vaccinees with a reporting delay in the VRS

The number of vaccinees reported in the VRS was expressed by using the discrete delay equation (TsuZuki et al., 2017) as follows:

$$c_{t,x} = j_t F_{x-t} \tag{1}$$

$$E(c_{t,x}) = \frac{c_{t,x'}}{F_{x'-t}} F_{x-t} \tag{2}$$

where $c_{t,x}$ is the number of people vaccinated on day t and reported on day x , and j_t represents the true number of people vaccinated on day t . We assumed that the proportion of vaccinees on day t who were reported by day x followed F_{x-t} , which is a cumulative distribution function of the delay and has a gamma distribution. The gamma distribution parameters were estimated through the maximum likelihood method and assuming that $c_{t,x}$ followed a Poisson distribution:

$$L(\theta; c_{t,x}) = \prod_{j=1}^{m-1} \prod_{t=1}^{x_j} \frac{E(c_{t,x_j})^{c_{t,x_j}} \exp(-E(c_{t,x_j}))}{c_{t,x_j}!} \tag{3}$$

where $E(\cdot)$ represents the expected number, x_j represents the date on which the VRS dataset was obtained, m is the dataset number ($m = 10$ snapshots), and θ represents the population parameter governing the gamma distribution. To quantify the uncertainty of the parameters, a parametric bootstrap method was employed, resampling 1,000 sets of parameters using a Hessian matrix. The number of vaccinees, j_t , was calculated, accounting for the estimated reporting delay.

In addition, underreported doses, which were recorded in the V-SYS only, were added to the number of vaccinees estimated previously under the assumption that the doses were administered after the age distribution of the working population according to the national statistics.

2.2.3. Estimating the age-specific fraction of people who are susceptible to infection

We assumed that increased vaccine effectiveness since the first vaccination follows a cumulative function for a Weibull distribution; thus, the cumulative number of people with immune protection against infection was calculated as:

$$I_{a,T} = VE \sum_{t=0}^T \sum_{\tau=1}^{t-1} j_{a,t-\tau} h_{\tau} \tag{4}$$

where $I_{a,T}$ represents the cumulative number of people immune to infection at time T in age group a , and VE is the maximum vaccination effectiveness, which we assumed to be 0.8 against infection

with the Delta variant (Sheikh et al., 2021), which was prevalent during the period of interest. Note that vaccine effectiveness here assumes “all or nothing” rather than “partial” or “leaky” protection mechanism, meaning that $I_{a,T}$ is the number of successfully immunized people (i.e., given VE, 20% of the vaccinated population would fail to acquire immunity that practically prevents infection). $j_{a,t-\tau}$ represents the number of newly vaccinated people in age group a on day $t - \tau$. h_τ is the Weibull distribution function, representing vaccine effectiveness against infection on day τ since receiving the first dose. Based on a previously published cohort study, which reported the cumulative number of the documented SARS-CoV-2 infection from the day of the first dose vaccination (Dagan et al., 2021), we estimated parameters for the Weibull distribution function as well as the probability of getting infected with SARS-CoV-2 during each fraction of the follow-up period through the maximum likelihood method, assuming that the incidence among vaccinated and unvaccinated population occurred after binomial distribution, that is,

$$L(\theta; unvac_{+ve,\tau}, unvac_{total,\tau}, vac_{+ve,\tau}, vac_{total,\tau}) = \prod_{\tau} \left(\frac{unvac_{total,\tau}}{unvac_{+ve,\tau}} \right)^{p unvac_{+ve,\tau}} (1-p)^{unvac_{total,\tau} - unvac_{+ve,\tau}} \left(\frac{vac_{total,\tau}}{vac_{+ve,\tau}} \right)^{p vac_{+ve,\tau}} (1-p)^{vac_{total,\tau} - vac_{+ve,\tau}} \quad (5)$$

where $unvac_{+ve,\tau}$ and $vac_{+ve,\tau}$ are the number of documented infections among unvaccinated and vaccinated population, respectively at time τ (i.e., days elapsed since receiving the first dose), whereas $unvac_{total,\tau}$ and $vac_{total,\tau}$ are the total number at risk during each fraction of follow-up period. τ was determined to be the median of each period at risk. We employed the bootstrapping method and derived 1,000 sample parameter sets from a Hessian matrix. It should be noted that this time-varying vaccine effectiveness since the first dose vaccination is based on the assumption that all of those who received the first dose vaccine would take the second dose on day 21 after the first dose. This assumption was deemed reasonable because the percentage of people who received the first dose but not second dose was only about 1% in Japan (Prime Minister's Office of Japan, 2022). The interpretation of the cumulative density function for the estimated Weibull distribution is therefore the vaccine effectiveness that increases over time since receiving the first dose and eventually plateaus at the maximum vaccine effectiveness of the second dose.

The number of immune individuals was converted into the fraction who were susceptible:

$$s_{a,T} = 1 - \frac{I_{a,T}}{N_a} \quad (6)$$

where $s_{a,T}$ represents the fraction of people susceptible to infection in age group a at time T , and N_a is the number of people in age group a . The 95% CIs for $s_{a,T}$ were computed by two sets of samples: parameters for the gamma distribution, representing the reporting delay in the VRS, and the Weibull distribution, representing the time-dependent vaccine effectiveness. This study monitored the immune landscape near the end of the two-dose program; for simplicity, we did not account for waning immunity.

2.2.4. Next-generation matrix

To investigate transmission across age groups, the NGM was employed (Kayano et al., 2019), and the time-varying reproduction number was computed as the largest eigenvalue of the NGM, $\{R_{ab}\}$, calculated as:

$$R_{ab} = k_a m_{ab} \quad (7)$$

where k_a is the relative susceptibility to infection through an effective contact with a COVID-19 case in age group a . m_{ab} is the contact rate between an infectee in age group a and an infector in age group b , obtained from a contact survey conducted in Japan

(Munasinghe et al., 2019), while we modified the matrix to be consistent with the previously mentioned five age groups. To estimate the relative susceptibility, the after renewal equation was employed:

$$c_{a,t} = \sum_{\tau=1}^{t-1} \sum_{b=1}^{n_a} R_{ab} u_{b,t-\tau} g_{\tau} \quad (8)$$

where $u_{a,t}$ represents the number of newly infected COVID-19 cases in age group a on day t , and g_{τ} is the probability mass function of the generation time. We quantified the NGM during the period in which the Alpha variant was initially present in Japan, using the confirmed case data (representing the incidence of symptom onset on day t) and the serial interval (Nishiura et al., 2020). As explained previously, R_{ab} is an element of the NGM $\{R_{ab}\}$. Fitting Equation (8) to the incidence data, the relative susceptibilities were estimated during the exponential growth phase in Osaka owing to the introduction of Alpha from March 1, 2021 to April 12, 2021. We assumed that the distribution of case counts by age group was sufficiently captured by a Poisson distribution, and the likelihood function was written as:

$$L(\theta; c_{a,t}) = \prod_t \prod_a \frac{E(u_{a,t})^{c_{a,t}} e^{-E(u_{a,t})}}{c_{a,t}!} \quad (9)$$

where $E(u_{a,t})$ represents the expected number of cases derived from the right-hand side of Equation (8). Minimizing the negative logarithm of Equation (9), we obtained the unknown parameter θ , i.e., $\{k_a\}$. The 95% CIs were calculated using parametric bootstrapping.

2.2.5. Time-dependent reproduction number

The time-dependent NGM reflects the immune landscape and was modeled as:

$$R_{ab,t}^v = s_{a,t} R_{ab} \quad (10)$$

where $s_{a,t}$ represents the fraction of people who are susceptible to infection in age group a at time t estimated from Equation (6), and R_{ab} is the NGM as derived from the Alpha variant epidemic. We set June 6, 2021 as the starting point for applying Equation (10); this day was just before vaccinations shifted from focusing on older people to the younger age groups. The relative reduction of the reproduction number was explored using the dominant eigenvalue of the time-dependent NGM over time. We used the R_{ab} from the Alpha variant epidemic, but the monitoring was carried out during the period when the Delta variant was dominant. We therefore further assessed an impact of the replacement of Alpha by Delta, by adjusting the estimated largest eigenvalues on the basis of the relative transmissibility of the variants (Ito et al., 2021).

Results

The V-SYS recorded 6,532,164 first dose vaccines allocated to healthcare workers between February 17, 2021 and July 30, 2021. The VRS recorded 87,700,381 vaccinees who received a first dose as a member of the general population, a university student/staff member, or a company employee between April 17, 2021 and October 17, 2021. In addition, the V-SYS recorded 1,123,840 first doses distributed through the university and workplace vaccination programs that were not counted in the VRS.

Figure 1 shows the number of people who received a first dose recorded in the VRS. The data show that many people who were vaccinated had their information updated in the VRS as time went on. For instance, from June, 2021 to September 2021, 3,500,000–4,000,000 first doses were administered per week according to the most recent data (updated October 17, 2021); this is compared with the 3,000,000–3,500,000 doses initially reported in real time.

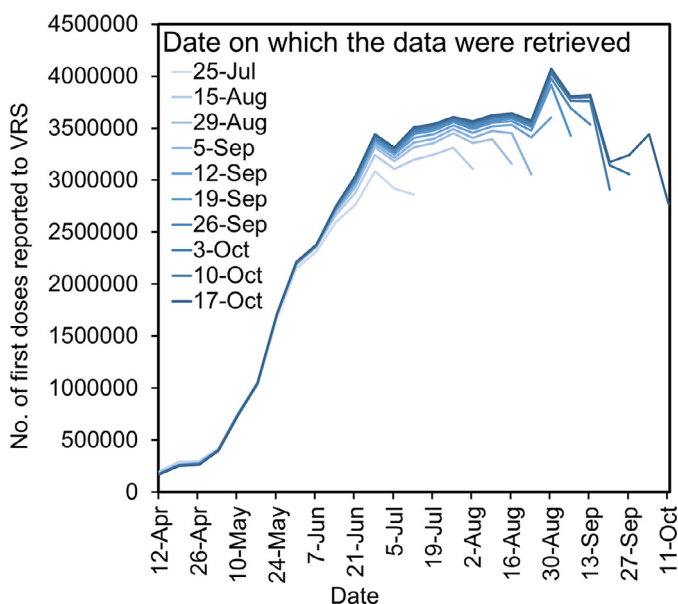


Figure 1. Weekly number who received the first dose between April 12, 2021, and October 17, 2021 (except for healthcare workers) according to the Vaccination Record System (VRS). The lines represent the number of vaccinees reported to VRS, indicating that some previously unreported vaccinees were included later as the data were updated.

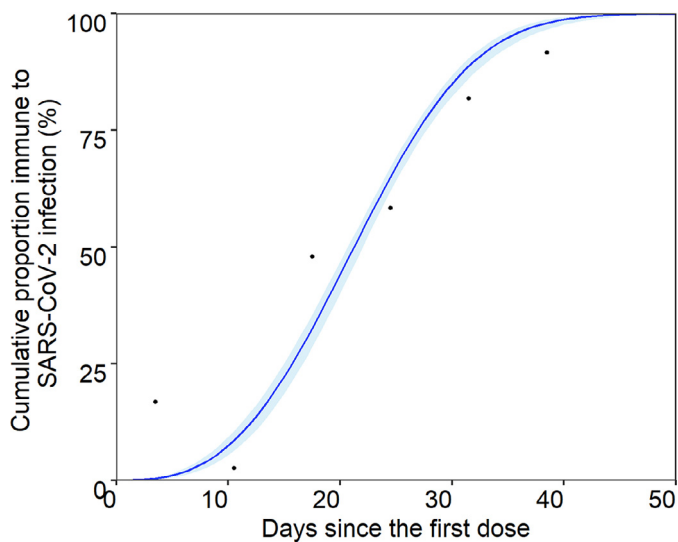


Figure 2. Delay while immune protection against SARS-CoV-2 infection builds up. The points represent empirically observed vaccine effectiveness against SARS-CoV-2 infection (Dagan et al., 2021). The line and shaded area show our estimate for the Weibull distribution and the 95% confidence intervals (CIs), respectively. The distribution applies to those who were successfully immunized (and protected) against infection. There would be a certain fraction of vaccination failures; these are not shown here but were included in our immune landscape calculations as *VE*.

Using 10 different datasets (i.e., 10 snapshot observations of the VRS data), the mean reporting delay was estimated to be 13.93 days (95% CI: 13.88–13.98).

Figure 2 shows the estimated time-dependent vaccine effectiveness since the first dose (i.e., the cumulative density function for the estimated Weibull distribution), based on a published cohort study (Dagan et al., 2021). The jointly estimated probability of getting infected with SARS-CoV-2 during the period of the cohort study was 0.0038 (95% CI: 0.0037– 0.0039), and the mean and SD of the cumulative Weibull distribution were estimated to be 21.49 days (95% CI: 20.80– 22.15) and 32.09 days (95% CI: 27.17–

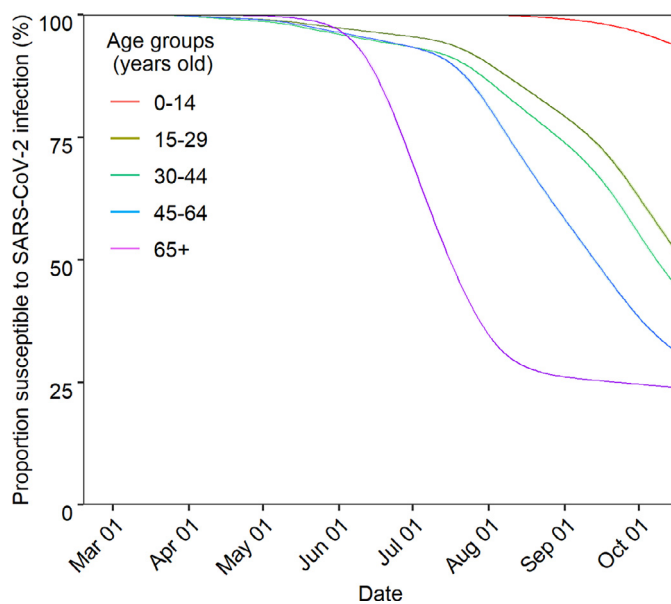


Figure 3. Age-specific proportion susceptible to SARS-CoV-2 infection from February 17, 2021, to October 17, 2021. The lines represent the proportion susceptible. The shaded areas indicate the 95% confidence intervals (CIs) based on the parametric bootstrap method.

39.17), respectively. That is, it was estimated to take approximately 20 days to reach 50% maximum vaccine effectiveness after the first dose.

Accounting for the reporting delays and the delay in vaccine effectiveness, the population fractions susceptible to COVID-19 infection on October 17, 2021 were estimated to be 93.55% (95% CI: 93.41– 93.70), 51.31% (95% CI: 50.84– 51.78), 44.23% (95% CI: 43.85– 44.65), 31.01% (95% CI: 30.78– 31.25), and 23.93% (95% CI: 23.89– 23.97), respectively, among people aged 0–14, 15–29, 30–44, 45–64, and ≥ 65 years (Figure 3; Supplementary data 2). The oldest group has the highest risk of severe disease (Jordan et al., 2020) but had the largest immune fraction. In contrast, a substantial fraction of younger adults and children remained susceptible as of October 17, 2021.

Relative susceptibility parameters were estimated to be 0.08 (95% CI: 0.07–0.08), 0.27 (95% CI: 0.26–0.28), 0.24 (95% CI: 0.23–0.25), 0.35 (95% CI: 0.33–0.36), and 0.27 (95% CI: 0.26–0.28) for individuals aged 0–14, 15–29, 30–44, 45–64, and ≥ 65 years, respectively. People aged 45–64 years had the highest susceptibility, whereas those who were younger than 15 had the lowest susceptibility. Figure 4 compares the observed and predicted number of confirmed COVID-19 cases in Osaka. The predicted age-dependent patterns were well captured overall and did not deviate from the observed counts. In addition, in the early stage of the Alpha epidemic from March 1 to April 12, 2021 in Osaka (which was unaffected by strong countermeasures such as a state of emergency declaration, which took place later), the largest estimated eigenvalue of the NGM was 1.39 (95% CI: 1.35–1.44).

Figure 5 shows the time-dependent eigenvalues of the NGM over the study period relative to the estimated value on June 6. The eigenvalues can be interpreted as the Alpha or Delta variant reproduction number, which explicitly accounted for an increasingly immune population owing to vaccination. As the immune fraction of the population increased, the reproduction numbers for Alpha decreased to 0.96 (95% CI: 0.92–1.01), 0.87 (95% CI: 0.83–0.92), 0.77 (95% CI: 0.73–0.80), and 0.62 (95% CI: 0.59–0.65) on July 18, August 15, September 12, and October 10, 2021, respectively. As being expected, the reproduction numbers for Delta was estimated to be substantially higher than that for Alpha, and they were 2.07 (95%

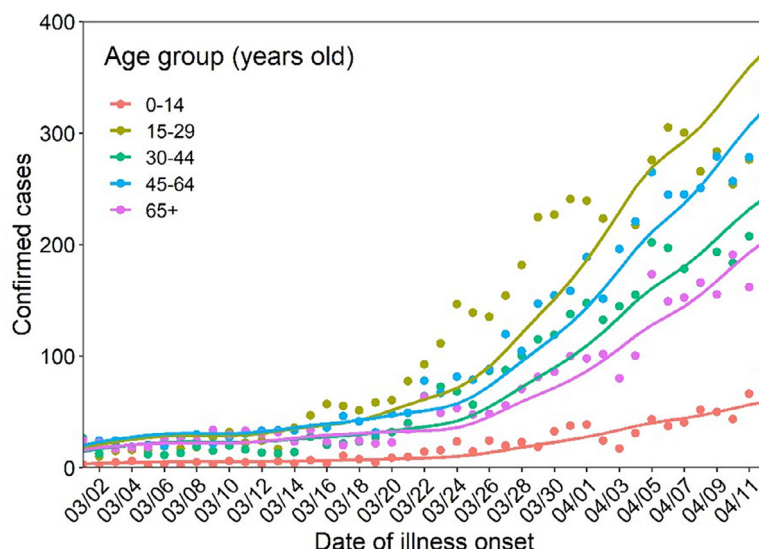


Figure 4. Comparison between the observed and predicted numbers of confirmed cases in Osaka from March 1, 2021, to April 12, 2021. The dots represent the daily confirmed cases of COVID-19 by age group in Osaka prefecture in the growth phase of the fourth wave, i.e., during the Alpha variant wave. The lines indicate the predicted daily confirmed cases of COVID-19 by age group in Osaka based on the maximum likelihood estimation that inferred the next-generation matrix.

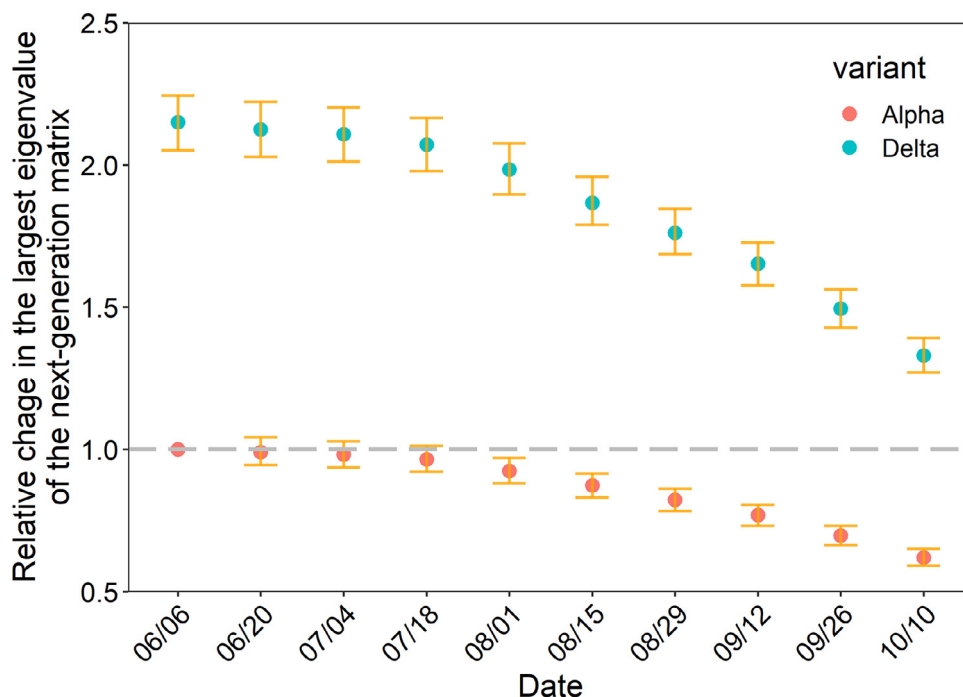


Figure 5. Relative value of the largest eigenvalue, as computed from the next-generation matrix covering Japan from June 6, 2021, to October 10, 2021. The relative changes in the largest eigenvalues of the next-generation matrix were explored. The baseline value was taken on June 6, 2021, and estimates were updated at two-week intervals. The green and red points represent the relative value of the largest eigenvalues for the Delta and Alpha variants, respectively. The gray dashed line indicates unity for the Alpha variant (i.e., the value of 1.0 below which the epidemic can be brought under control). The error bars represent the 95% confidence intervals based on the parametric bootstrap method.

CI: 1.98–2.16), 1.87 (95% CI: 1.79–1.96), 1.65 (95% CI: 1.57–1.72), 1.33 (95% CI: 1.27–1.39) for the same date as previously mentioned.

Discussion

We provided a real-time estimate of the fraction of the Japanese population susceptible to SARS-CoV-2 infection while addressing two important delay distributions: (i) reporting delays in the vaccine registration systems and (ii) the time required for vaccinated individuals to become immune to infection. We estimated an approximately 2-week reporting delay in the VRS. Furthermore, it

takes approximately 3 weeks for 50% of successfully vaccinated people to become immune to infection after receiving the first dose. The susceptible proportion was much higher in younger and more socially active age groups. Of those aged 15–29 years, more than 90% were still susceptible to infection at the end of the study period, in contrast with approximately 20% of those aged ≥ 65 . The time-dependent reduction in the susceptible fraction strongly contributed to reducing the reproduction number. By the end of the study period, the reproduction number was reduced by approximately 40% regardless of the variant of interest compared with before the vaccines became widely available.

By accounting for the two sources of delay, the present study allowed real-time monitoring of the COVID-19 immune landscape using vaccine registration datasets. The reporting delay can be substantial, especially when a new registration system is launched, which was the case for the systems used in Japan. Furthermore, it can take weeks after vaccination to develop immune protection against infection, and some people will be susceptible during this time. If the reported vaccination coverage is regarded as equal to population immunity, it would be an overestimation and could potentially create a false sense of security. The timely estimation of the fraction susceptible to infection enabled us to monitor the relative change in the effective reproduction number that was solely attributable to vaccination. Our framework clarified the population impacts of vaccination and was used to evaluate the vaccination campaign in a low-incidence country. To our knowledge, this is the first study to report monitoring the immune landscape based on data from vaccine registration systems.

The fraction of the population susceptible to COVID-19 infection considerably varied by age. One reason for the variation was the prioritization of vaccination order by age (Jordan et al., 2020). Older people became eligible earlier than younger people. Higher vaccination coverage was achieved in the older age groups, perhaps because they are at higher risk of severe disease and death. In contrast, not all young adults have yet received a first dose, and most remained susceptible to infection throughout the study period. Vaccine hesitancy may also have contributed to variations in susceptibility by age. According to a nationwide cross-sectional survey in Japan, young people were more likely to be hesitant to get a COVID-19 vaccination (Okubo et al., 2021). However, young adults also tend to have more contacts, which drives transmissions (Mossong et al., 2008) and can contribute to mismatches between the individual and public benefits of vaccination.

Here, we combined immune landscape monitoring with the effective reproduction number to account for the vaccine-induced reduction in the susceptible fraction of the population in real time. By employing an NGM, the fraction of the population immune to infection and the transmission dynamics over time were quantitatively assessed, showing that vaccination contributed to a substantial decrease in the reproduction number. The present study explored the immune landscape toward the end of the second-dose campaign; thus, for simplicity, we did not account for waning immunity. The intrinsic mechanism of waning, booster dose vaccination, and exposure to infectious individuals during the protected period would complicate the immune fraction computation, and we will examine these impacts in the future study.

This study has some limitations. First, we assumed that vaccine effectiveness was identical in all age groups. However, given that the immunogenicity after vaccination with BNT162b2 can differ by age (Abu Jabal et al., 2021), the time delay between vaccination and becoming immune and the vaccine efficacy might vary with age. Second, our model relied on published values of BNT162b2 effectiveness (Dagan et al., 2021). However, a small fraction of people received the mRNA-1273 or ChAdOx1-S vaccine, and they were assumed to have had the same benefit as those who received BNT162b2. The true differences in benefit were deemed negligible because the mRNA vaccines showed similar efficacy in the initial vaccine trials (Baden et al., 2021; Polack et al., 2020), and only 0.06% of the population received a first dose of ChAdOx1-S (Prime Minister's Office of Japan, 2022). Third, we did not use the data on the number of people who were fully vaccinated. However, we believe that our approach with focus on the first dose vaccination provided more precise immune landscape, given the rapidly growing number of the first-dose vaccinees, because the immunity should start building up upon the first dose vaccination. Moreover, the estimated time-dependent vaccine effectiveness incorporates the effectiveness of second dose vaccination because of

our assumption that all individuals who received the first dose will take the second dose. As briefly mentioned earlier, we considered this assumption reasonable because it was reported that there is only 1% of people who did not take the second dose among those who were vaccinated with the first dose. Fourth, to estimate the susceptibilities in the NGM, we used the data on COVID-19 cases when the Alpha variant was dominant; however, it had been replaced by Delta when we estimated the NGM (Ministry of Health, Labor and Welfare, 2021b). It was not feasible to estimate the susceptibilities during the time that Delta was dominant because the vaccination coverage had rapidly increased. Thus, we instead examined the impact of Delta by accounting for the relative transmissibility of Delta to that of Alpha. Finally, the contact matrix we used in the NGM was estimated before the pandemic started, and it might have differed from the contact patterns at the time of the study owing to the considerable behavior changes associated with the PHSMs and people's perceptions of COVID-19 risk.

Despite these avenues for future improvement, the present study offers a novel approach to monitoring the age-related immune landscape over time in Japan. By accounting for reporting delays and the time required to build immunity, our calculations provided fundamental insights into COVID-19 protection at a population level. Moreover, our framework can be easily extended to include other sophisticated analyses such as monitoring herd immunity by measuring the reproduction number under additional vaccination scenarios (e.g., vaccination among children).

Conflict of interest

The authors have no competing interests to declare.

Funding sources

HN received funding from Health and Labour Sciences Research Grants (20CA2024, 20HA2007, 21HB1002, and 21HA2016); the Japan Agency for Medical Research and Development (JP20fk0108140, JP20fk0108535, and JP21fk0108612); the Japan Society for the Promotion of Science (JSPS) KAKENHI (21H03198); the Environment Research and Technology Development Fund (JP-MEERF20S11804) of the Environmental Restoration and Conservation Agency of Japan; and the Japan Science and Technology Agency SICORP program (JPMJSC20U3 and JPMJSC2105). TK received funding from the JSPS KAKENHI (21K10495).

Ethical approval statement

The present study used publicly available data from the Ministry of Health, Labor and Welfare, and all data were de-identified before analysis. This study was approved by the Medical Ethics Board of the Graduate School of Medicine, Kyoto University (R2676).

Acknowledgments

We thank the local governments, public health centers, and institutes for surveillance, laboratory testing, epidemiological investigation, and data collection. We thank Edanz (<https://jp.edanz.com/ac>) for editing a draft of this manuscript. The funders had no role in study design, data collection and analysis, decision to publish, or preparation of the manuscript.

Supplementary materials

Supplementary material associated with this article can be found, in the online version, at [doi:10.1016/j.ijid.2022.06.005](https://doi.org/10.1016/j.ijid.2022.06.005).

References

- Abu Jabal KA, Ben-Amram H, Beirut K, Batheesh Y, Sussan C, Zarka S, et al. Impact of age, ethnicity, sex and prior infection status on immunogenicity following a single dose of the BNT162b2 mRNA COVID-19 vaccine: real-world evidence from healthcare workers, Israel, December 2020 to January 2021. *Euro Surveill* 2021;26:1–5.
- Andrews N, Stowe J, Kirsebom F, Toffa S, Rickeard T, Gallagher E, et al. Covid-19 vaccine effectiveness against the omicron (B.1.1.529) variant. *N Engl J Med* 2022;386:1532–46.
- Baden LR, El Sahly HM, Essink B, Kotloff K, Frey S, Novak R, et al. Efficacy and safety of the mRNA-1273 SARS-CoV-2 vaccine. *N Engl J Med* 2021;384:403–16.
- Belay ED, Godfred-Cato S. SARS-CoV-2 spread and hospitalisations in paediatric patients during the omicron surge. *Lancet Child Adolesc Health* 2022;6:280–1.
- Berselli N, Filippini T, Paduano S, Malavolti M, Modenese A, Gobba F, et al. Seroprevalence of anti-SARS-CoV-2 antibodies in the Northern Italy population before the COVID-19 second wave. *Int J Occup Med Environ Health* 2022;35:63–74.
- Chemaitelly H, Yassine HM, Benslimane FM, Al Khatib HA, Tang P, Hasan MR, et al. mRNA-1273 COVID-19 vaccine effectiveness against the B.1.1.7 and B.1.351 variants and severe COVID-19 disease in Qatar. *Nat Med* 2021;27:1614–21.
- Chung H, He S, Nasreen S, Sundaram ME, Buchan SA, Wilson SE, et al. Effectiveness of BNT162b2 and mRNA-1273 COVID-19 vaccines against symptomatic SARS-CoV-2 infection and severe COVID-19 outcomes in Ontario, Canada: test negative design study. *BMJ* 2021;374:n1943.
- Dagan N, Barda N, Kepten E, Miron O, Perchik S, Katz MA, et al. BNT162b2 mRNA COVID-19 vaccine in a nationwide mass vaccination setting. *N Engl J Med* 2021;384:1412–23.
- Elbe S, Data Buckland-Merrett G. disease and diplomacy: GISAID's innovative contribution to global health. *Glob Chall* 2017;1:33–46.
- Ferdinands JM, Rao S, Dixon BE, Mitchell PK, DeSilva MB, Irving SA, et al. Waning 2-dose and 3-dose effectiveness of mRNA vaccines against COVID-19-associated emergency department and urgent care encounters and hospitalizations among adults during periods of delta and omicron variant predominance – VISION network, 10 states, August 2021–January 2022. *MMWR Morb Mortal Wkly Rep* 2022;71:255–63.
- GISAID, 2022. <https://www.gisaid.org> (accessed 15 June 2022)
- Haas EJ, Angulo FJ, McLaughlin JM, Anis E, Singer SR, Khan F, et al. Impact and effectiveness of mRNA BNT162b2 vaccine against SARS-CoV-2 infections and COVID-19 cases, hospitalisations, and deaths following a nationwide vaccination campaign in Israel: an observational study using national surveillance data. *Lancet* 2021;397:1819–29.
- Hall VJ, Foulkes S, Saei A, Andrews N, Oguti B, Charlett A, et al. COVID-19 vaccine coverage in health-care workers in England and effectiveness of BNT162b2 mRNA vaccine against infection (SIREN): a prospective, multicentre, cohort study. *Lancet* 2021;397:1725–35.
- Houhamdi L, Gautret P, Hoang VT, Fourmier PE, Colson P, Raoult D. Characteristics of the first 1119 SARS-CoV-2 Omicron variant cases, in Marseille, France, November–December 2021. *J Med Virol* 2022;94:2290–5.
- Ito K, Piantham C, Nishiura H. Predicted dominance of variant Delta of SARS-CoV-2 before Tokyo Olympic Games, Japan, July 2021. *Euro Surveill* 2021;26.
- Jentsch PC, Anand M, Bauch CT. Prioritising COVID-19 vaccination in changing social and epidemiological landscapes: a mathematical modelling study. *Lancet Infect Dis* 2021;21:1097–106.
- Jordan RE, Adab P, Cheng KK. COVID-19: risk factors for severe disease and death. *BMJ* 2020;368:m1198.
- Kayano T, Lee H, Nishiura H. Modelling a supplementary vaccination program of rubella using the 2012–2013 epidemic data in Japan. *Int J Environ Res Public Health* 2019;16.
- Loconsole D, Biscaglia L, Centrone F, Sallustio A, Accogli M, Dalfino L, et al. Autochthonous outbreak of SARS-CoV-2 omicron variant in booster-vaccinated (3 doses) healthcare workers in Southern Italy: just the tip of the iceberg? *Vaccines* 2022;10:1–9.
- Madhi SA, Kwatra G, Myers JE, Jassat W, Dhar N, Mukendi CK, et al. Population immunity and COVID-19 severity with omicron variant in South Africa. *N Engl J Med* 2022;386:1314–26.
- Mathieu E, Ritchie H, Ortiz-Ospina E, Roser M, Hasell J, Appel C, et al. A global database of COVID-19 vaccinations. *Nat Hum Behav* 2021;5:947–53.
- Ministry of Health, Labour and Welfare, 2021a. *The situation analysis on COVID-19 and response from MHLW*, December 31, 2021. https://www.mhlw.go.jp/stf/newpage_23137.html (accessed 15 June 2022)
- Ministry of Health, Labour and Welfare, 2021b. *Advisory board for COVID-19 control, 50th*. https://www.mhlw.go.jp/stf/seisakunitsuite/bunya/0000121431_00294.html (accessed 15 June 2022)
- Mossong J, Hens N, Jit M, Beutels P, Auranen K, Mikolajczyk R, et al. Social contacts and mixing patterns relevant to the spread of infectious diseases. *PLoS Med* 2008;5:e74.
- Munasinghe L, Asai Y, Nishiura H. Quantifying heterogeneous contact patterns in Japan: a social contact survey. *Theor Biol Med Model* 2019;16:6.
- National Institute of Infectious Diseases, 2021. *About new concerning variant of SARS-CoV-2 that may have different infectiousness, transmissibility, and antigenicity (9th report)*. <https://www.niid.go.jp/niid/ja/2019-ncov/2484-idsc/10434-covid19-43.html>. (accessed 15 June 2022)
- Nishiura H, Linton NM, Akhmetzhanov AR. Serial interval of novel coronavirus (COVID-19) infections. *Int J Infect Dis* 2020;93:284–6.
- Nopsopon T, Pongpirul K, Chotirosniramit K, Jakaew W, Kaewwijit C, Kanchana S, et al. Seroprevalence of hospital staff in a province with zero COVID-19 cases. *PLoS ONE* 2021;16.
- Nyberg T, Ferguson NM, Nash SG, Webster HH, Flaxman S, Andrews N, et al. Comparative analysis of the risks of hospitalisation and death associated with SARS-CoV-2 omicron (B.1.1.529) and delta (B.1.617.2) variants in England: a cohort study. *Lancet* 2022;399:1303–12.
- Okubo R, Yoshioka T, Ohfujii S, Matsuo T, Tabuchi T. COVID-19 vaccine hesitancy and its associated factors in Japan. *Vaccines* 2021;9:1–10.
- Polack FP, Thomas SJ, Kitchin N, Absalon J, Gurtman A, Lockhart S, et al. Safety and efficacy of the BNT162b2 mRNA COVID-19 vaccine. *N Engl J Med* 2020;383:2603–15.
- Prime Minister's Office of Japan, 2022. *About COVID-19 vaccination 2022*, <https://www.kantei.go.jp/jp/headline/kansensho/vaccine.html>. (accessed 15 June 2022)
- Pritchard E, Matthews PC, Stoesser N, Eyre DW, Gethings O, Vihta KD, et al. Impact of vaccination on new SARS-CoV-2 infections in the United Kingdom. *Nat Med* 2021;27:1370–8.
- Ramírez JD, Castañeda S, Ballesteros N, Muñoz M, Hernández M, Banu R, et al. Hotspots for SARS-CoV-2 omicron variant spread: lessons from New York City. *J Med Virol* 2022;94:2911–14.
- Sasanami M, Kayano T, Nishiura H. The number of COVID-19 clusters in healthcare and elderly care facilities averted by vaccination of healthcare workers in Japan, February–June 2021. *Math Biosci Eng* 2022;19:2762–73.
- Sheikh A, McMenamin J, Taylor B, Robertson C. Public Health Scotland and the EAVE II Collaborators. SARS-CoV-2 Delta VOC in Scotland: demographics, risk of hospital admission, and vaccine effectiveness. *Lancet* 2021;397:2461–2.
- Slot E, Hogema BM, Reusken CBEM, Reimerink JH, Molier M, Karregat JHM, et al. Low SARS-CoV-2 seroprevalence in blood donors in the early COVID-19 epidemic in the Netherlands. *Nat Commun* 2020;11:5744.
- Thompson MG, Burgess JL, Naleway AL, Tyner HL, Yoon SK, Meece J, et al. Interim estimates of vaccine effectiveness of BNT162b2 and mRNA-1273 COVID-19 vaccines in preventing SARS-CoV-2 infection among health care personnel, first responders, and other essential and frontline workers – eight US locations, December 2020–March 2021. *MMWR Morb Mortal Wkly Rep* 2021;70:495–500.
- Tseng HF, Ackerson BK, Luo Y, Sy LS, Talarico CA, Tian Y, et al. Effectiveness of mRNA-1273 against SARS-CoV-2 Omicron and Delta variants. *Nat Med* 2022;28:1063–71.
- Tsuzuki S, Lee H, Miura F, Chan YH, Jung SM, Akhmetzhanov AR, et al. Dynamics of the pneumonic plague epidemic in Madagascar, August to October 2017. *Euro Surveill* 2017;22:1–6.
- Veneti L, Boås H, Bråthen Kristoffersen A, Stålcrautz J, Bragstad K, Hungnes O, et al. Reduced risk of hospitalisation among reported COVID-19 cases infected with the SARS-CoV-2 Omicron BA.1 variant compared with the Delta variant, Norway, December 2021 to January 2022. *Euro Surveill* 2022;27.
- Xu X, Sun J, Nie S, Li H, Kong Y, Liang M, et al. Seroprevalence of immunoglobulin M and G antibodies against SARS-CoV-2 in China. *Nat Med* 2020;26:1193–5.